The average energy, which was evaluated by using the expression for F_0 as given in Eq. (19) and using the generating function for the Laguerre polynomials, can be expressed to first order in K^2 as

$$\epsilon_{av}=\tfrac{3}{2}kT(1-0.30K^2).$$

The accuracy of the numerical constant appearing in this expression is about 1%. As in the case for constant collision frequency, we again see that the average energy is lower than the thermal energy of the gas. The deviation of the electron energy away from the thermal value can be put in the following form

$$\delta\epsilon/\epsilon_{gas}=-(\beta d_\epsilon/d)^2,$$

where d_ϵ, the characteristic energy decay distance, is

$$d_\epsilon=\pi\left(\frac{M}{6m}\right)^{1/2}\frac{1}{N\sigma}(0.55),$$

and d is the distance between the planes. For example, d_ϵ for He can be expressed as

$$d_\epsilon^{He}=\left(\frac{3.7}{Pd}\right)^2,$$

where σ is taken as 5.0×10^{-16} cm^2 [9] and P is the pressure expressed in mm Hg at 300°K. If we take $d=1$ cm, $P=10$ mm, and $\beta=1$ (lowest spatial mode), then

$$\delta\epsilon/\epsilon_{gas}=-0.14.$$

We again see, as in the case for constant ν, that as $\lambda\rightarrow0$ the expressions for the time constant and the average energy approach the equilibrium values with

$$\text{time constant}\rightarrow(d/\beta\pi)^2(1/D_\sigma),$$

where

$$D_\sigma=(2kT/m\pi)^{1/2}(2\lambda/3),$$

and

$$\epsilon_{av}\rightarrow\tfrac{3}{2}kT.$$

[9] L. S. Frost and A. V. Phelps, Phys. Rev. **136**, A1538 (1964).

PHYSICAL REVIEW VOLUME 139, NUMBER 6A 13 SEPTEMBER 1965

Nanosecond-Pulse Breakdown in Gases*

PETER FELSENTHAL† AND JOSEPH M. PROUD‡
Space Sciences, Incorporated, Waltham, Massachusetts
(Received 29 April 1965)

A theory describing the formative period of breakdown in gases following the sudden application of a dc electric field has been developed and applied to the design of experiments to measure lag times in nine gases. It is shown analytically that under certain conditions pulsed-dc and pulsed-microwave breakdown are directly comparable. A pulsed-dc experimental system is described which permits measurements of the formative period over a wide range of applied field, gas pressure, and gap space. For those gases where sufficient basic data are available, theoretical and experimental results are in good agreement.

INTRODUCTION

THE electrical breakdown of a gas is, in general, characterized by the net buildup of ionization from processes within the gas and from a host of secondary processes at walls and electrodes of the discharge vessel. Under certain conditions it has been possible to investigate breakdown with cw microwave techniques[1–3] where the electron generation and loss mechanisms are confined to the gas alone. The applicable diffusion theory then accounts for the balance between impact ionization as the generation process and attachment and diffusion as the loss processes. The validity of the diffusion theory[3] is subject to requirements on field uniformity, electron mean free path, and the amplitude of electron oscillation in the alternating field. The same theory has been applied successfully to the investigation of the formative time for breakdown under pulsed-microwave conditions.[4] An additional simplification can be achieved in this case since it is possible to design experiments in which the diffusion loss of electrons is negligible.

The research described in this paper was undertaken with the premise that the restriction of breakdown processes to those taking place in the gas could also be achieved under pulsed-dc breakdown conditions. Under these conditions the formative processes of breakdown can be described within the same theoretical framework as employed in microwave breakdown, and the experimental results for the two types of break-

* This research was supported by Rome Air Development Center, Rome, New York.
† Now with Arthur D. Little Inc., Cambridge, Massachusetts.
‡ Now with Ikor Inc., Burlington, Massachusetts.
[1] A. D. MacDonald and S. C. Brown, Phys. Rev. **75**, 411 (1949).
[2] M. A. Herlin and S. C. Brown, Phys. Rev. **74**, 291 (1948).
[3] S. C. Brown and A. D. MacDonald, Phys. Rev. **76**, 1629 (1949).
[4] L. Gould and L. W. Roberts, J. Appl. Phys. **27**, 1162 (1956).

down are unified. Moreover, the pulsed-dc methods materially extend the range of breakdown parameters beyond that previously studied, especially where high electric-field values are required for breakdown.

THEORY

In taking this approach, we have departed somewhat from conventional descriptions of the formative processes in dc breakdown. In the investigation of formative lag in overvolted atmospheric gaps, Fletcher[5] analysed his results in terms of a streamer model of the breakdown process. Following a suggestion of Raether,[6] Fletcher computed the formative time as the time for an initial electron avalanche to build up a space-charge field comparable to the applied field. Dickey[7] later showed that a simpler calculation of the breakdown times reported by Fletcher could be formulated by discarding the streamer model and by estimating the growth rate of ionization and subsequent charge separation in the undistorted applied field. This approach not only yields reasonable agreement for the formative time, but also explains the observed pulse shapes just following breakdown. In the theory employed in our investigation we also consider the field to be undistorted by space charge during the development of breakdown just as in the microwave breakdown theory.[2] The limits of the theory for effectively electrodeless dc-pulse breakdown are then derived in a manner which is closely analogous to the development of validity limits for the diffusion theory of microwave breakdown. The limits so defined are then at once the limits for validity of theory and the limits within which experimental results using dc-pulse technique are comparable to those which might be obtained by microwave methods.

The experimental model on which the theory is based is one in which a voltage pulse is instantaneously applied to a gas contained between effectively infinite parallel-plate electrodes. It is assumed that the statistical lag component of the breakdown lag is eliminated by ensuring that a supply of initial electrons exists at the instant the overvoltage is applied. The formative lag time is then the measured characteristic time for buildup of ionization in the gap space. The appropriate form of the electron continuity equation which relates the net rate of change of electron density to the generation and loss mechanisms is then

$$\partial n/\partial t = \nu_i n - \nu_a n - \nabla\cdot\Gamma, \tag{1}$$

where n is the electron density, ν_i is the ionization frequency, ν_a is the attachment frequency, and Γ is the particle flow. In general, Γ will consist of diffusion and mobility components. However, to achieve effectively electrodeless conditions we must establish experimental design requirements such that the electron current does not lead to wall or electrode interactions within the time of interest. This is equivalent to the requirement that the term $\nabla\cdot\Gamma$ be neglected in Eq. (1). Since the mobility term will dominate in the pulsed-dc case, the condition which permits the neglect of this term is similar to that imposed by the oscillation amplitude limit in the case of microwave breakdown theory.

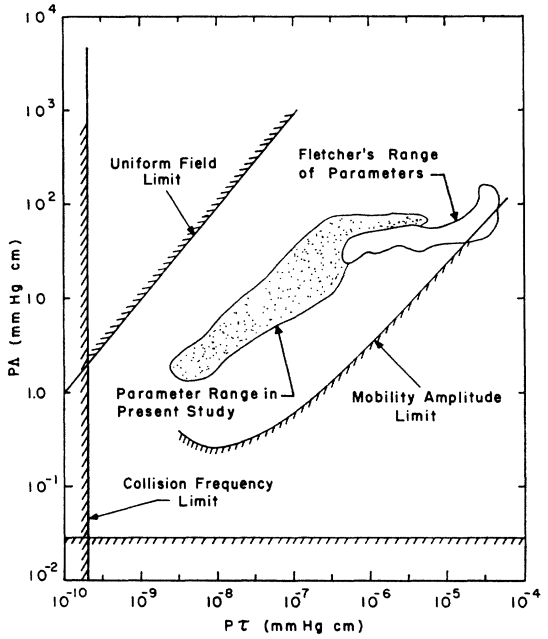

FIG. 1. Validity-limit lines for air compared with the range of parameters used in this study and in Fletcher's study.

To evaluate this and other limits of the theory as applied to pulsed-dc breakdown, it is useful to choose the following set of variables

$$P\tau, \quad P\Lambda, \quad E/P,$$

where P is the gas pressure, τ is the formative time, E is the applied field, and Λ is the characteristic diffusion length. For infinite parallel-plate geometry, $\Lambda = d/\pi$, where d is the plate separation. The limits which must be imposed may now be conveniently presented in the $P\Lambda$-$P\tau$ plane. The mobility-amplitude limit may be expressed by equating the plate separation to the electron drift distance during the formative period. In terms of the above variables we obtain

$$P\Lambda = \pi^{-1}k(E/P)\times P\tau, \tag{2}$$

where k is the product of electron mobility and the pressure. The limit line is developed empirically from the formative-time data which provide the values of E/P and $P\tau$ to be used.

If the formative time is short compared to the time of propagation of the voltage pulse across the gap, uniform-field conditions will not exist. Hence, the

[5] R. C. Fletcher, Phys. Rev. **76**, 1501 (1949).
[6] H. Raether, Elektrotech. Z. **63**, 301 (1942).
[7] F. R. Dickey, J. Appl. Phys. **23**, 1336 (1952).

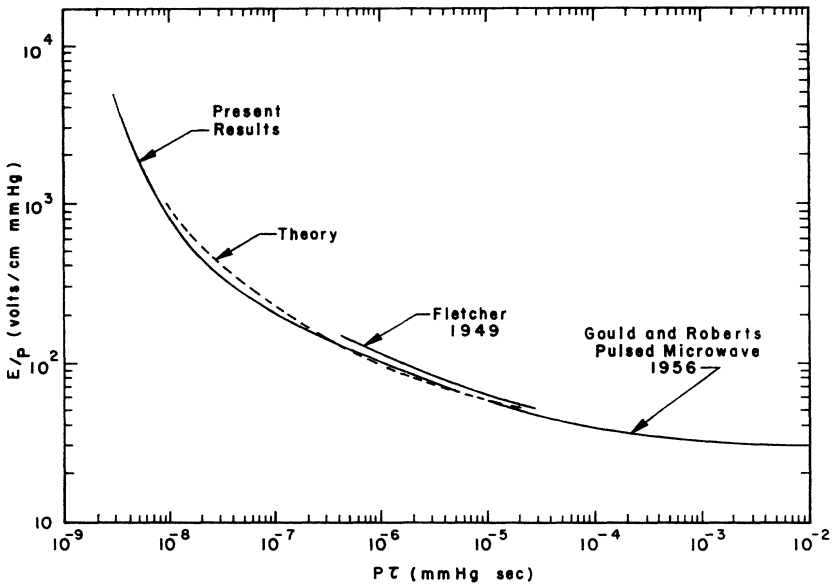

FIG. 2. Formative-time measurements in air compared with theory and data reported by previous investigators.

uniform-field limit is expressed by

$$P\Lambda = (c/\pi) \times P\tau, \tag{3}$$

where c is the wave velocity in the gap. As will be seen by examples below, the limit lines represented by Eqs. (2) and (3) are the important boundaries for validity of the theory. However, two additional considerations are noteworthy concerning the mean free path and the collision frequency. The mean-free-path limit arises when the mean free path is comparable to the gap separation, or

$$P\Lambda = 1/P_c, \tag{4}$$

where P_c is the probability of collision. Assuming a constant value for P_c, the limit line is a horizontal line in the lower portion of the $P\Lambda$-$P\tau$ plane.

The situation in which a rapid buildup of ionization occurs by impact ionization clearly requires many collisions during the pulse length, and one does not expect to observe breakdown by this process in time scales which are comparable to the mean collision time. Therefore, we shall always be concerned with conditions for which many collisions occur within the formative time. In this sense, it is proper to consider a collision-frequency limit defined by

$$P\tau = P/\nu_c, \tag{5}$$

where ν_c is the collision frequency.

The four limit lines are illustrated for air breakdown in Fig. 1. The portion of the plane bounded by the uniform-field limit on the left and the mobility-amplitude limit on the right is then the region within which the breakdown mechanisms are dominated by gaseous processes in uniform applied fields. In reality, of course, the boundaries indicated cannot be construed as precise since certain arbitrary choices of parameters have been exercised in Eqs. (2) through (5) and electron distributions have been ignored in favor of dealing with average electron behavior.

The breakdown parameters employed in the experiments for air reported below were located within a zone substantially removed from each limit line. This zone is indicated by the large shaded area in Fig. 1. For the other gases studied similar zones were established in the $P\Lambda$-$P\tau$ plane. The range of parameters associated with Fletcher's measurements in atmospheric gaps is also shown in the figure. The location of his breakdown parameters is near the mobility-amplitude-limit line suggesting that electrode processes played a role in the formative lag times which he measured.

With the neglect of the drift-loss term, Eq. (1) integrates to

$$\ln(n_b/n_0) = (\nu_i - \nu_a), \tag{6}$$

where n_b/n_0 is the ratio of the breakdown electron density to the initial density. The ionization and attachment frequency may be written in terms of the Townsend first ionization coefficient α, the attachment coefficient β, and the drift velocity $k(E/P)$ to yield

$$P\tau = \frac{\ln(n_b/n_0)}{k(E/P)(\alpha/P - \beta/P)}. \tag{7}$$

Use has been made of this expression with available data for k, α/P, and β/P to formulate the predicted curves of E/P versus $P\tau$ for each of the gases studied. The extent of the available data and the extrapolation techniques are discussed in Appendix I.

Equation (7) is plotted for air in Fig. 2 and compared with Fletcher's data, with microwave results

obtained by Gould and Roberts and with the average experimental curve obtained in this investigation. The generally good agreement between theory and experiment and the fact that the microwave and dc-pulse data are in accord with the same theory appear to support the approach taken as developed above.

APPARATUS

A high-voltage transmission-line system similar to that developed by Fletcher[8] was employed, yielding a wide range of the breakdown parameters, while maintaining an over-all time resolution of less than 1 nsec. The present system design departs from that of Fletcher's apparatus in the capability for pressure variation within the test gap and in the method for electrical observation of the breakdown lag time. The system illustrated in Fig. 3 develops variable pulse amplitudes of 4 to 30 kV with rise time as short as 0.3 nsec. It also provides an attenuated sample of the pulse for measurement of breakdown times, appropriate triggers, and a source of ultraviolet light for illumination of the test gap.

The main pulse generator is a high-pressure coaxial three-ball gap used to discharge a 60-nsec length of RG-17 cable. The two outer balls may be moved axially relative to the fixed center ball. The gap is of tapered 52-Ω coaxial construction with a small pulse-shaping condensor incorporated in the charging-line side of the gap. Gas pressure and ball-gap distance are adjusted to give proper operation at various cable charge voltages. Nitrogen or argon with pressures from 80 to 200 psi (gauge) is used as the insulating gas.

Pulse-shape observations are made by means of a coaxial current-viewing resistor of 0.212 Ω.[9] The resistor output is passed through a 4-Gc/sec bandwidth coaxial pad of 6, 10, or 13 dB and then to a 3-dB power divider and a matching transformer for the 125-Ω oscilloscope deflection system. The other output of the power

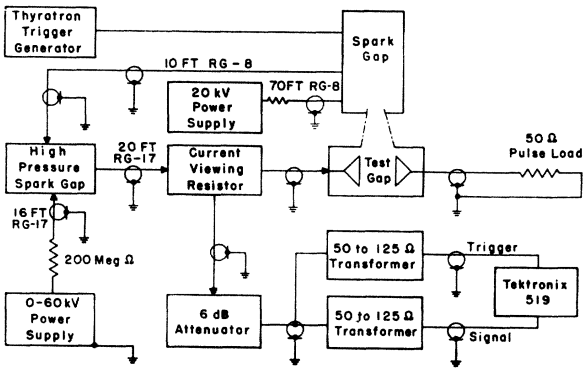

FIG. 3. Schematic diagram of experimental apparatus used for this study.

[8] R. C. Fletcher, Rev. Sci. Instr. **20**, 861 (1949).
[9] Supplied by T & M Research Products, Albuquerque, New Mexico.

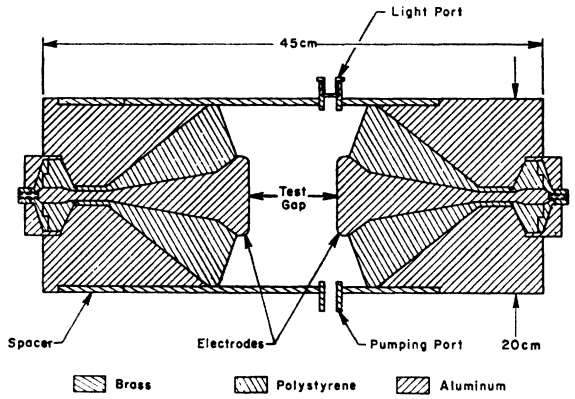

FIG. 4. Cross section of large test gap used in formative-time measurements.

divider is used to trigger the oscilloscope. A Tektronix 519 oscilloscope with a deflection sensitivity of 9.8 V/cm and rise time of 0.29 nsec is used to view the signals. With the aid of ASA 10 000 Polaroid film and an image reduction of 2:1, single trace photographs at 2 nsec/cm may be obtained.

In addition to the current-viewing resistor, the transmission line connecting the pulse generator and the test gap contains a 10-MΩ resistor between the center and outer conductors to dissipate any net charge left on this portion of the system after the high-voltage pulse has been applied to the test gap. A 50-Ω termination on the far side of the test gap provides a matched load for pulses transmitted through the gap when breakdown occurs.

The system trigger and ultraviolet illumination for the cathode are provided by the charged length of RG-8 cable. A low-voltage pulse is used to start the discharge of a ball-to-plane-to-point air gap. A first surface, 2.5-cm focal-length mirror is used behind the plane-to-point discharge to focus the light output on the cathode of the test gap. The high-voltage pulse from this discharge is used to trigger the pulse generator.

Two different test gaps have been used in the measurements reported here. Both gaps are basically the same tapered, 50-Ω coaxial construction. Polystyrene was used as the insulating material because of its low and uniform dissipation factor over the range of frequencies contained in the pulse. Both gaps have quartz windows for the admission of ultraviolet light to the cathode surface, ports for the admission of the test gases, and pumping ports. Polished aluminum electrodes with Rogowski contours[10] are used to provide uniform field conditions. The small gap is approximately 7.6-cm inside diameter with electrodes of 3.5-cm diameter. The gap distance is adjustable by means of a 20 turns per inch thread. Gap distances of 0.051 to 0.5 cm are used. The large gap shown in Fig. 4 is

[10] W. Rogowski and H. Rengier, Arch. Elektrotech. **16**, 73 (1926).

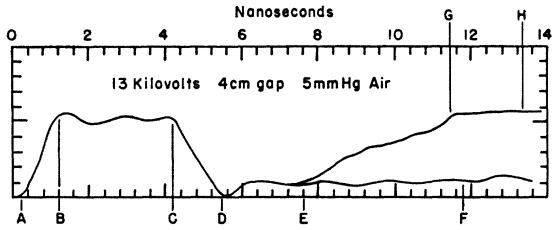

FIG. 5. Typical voltage waveform illustrating measurement technique.

approximately 20.2-cm inside diameter with electrodes of 8.0-cm diameter. Fixed spacers are used to provide gap distances of 2.0, 4.0, and 6.0 cm. The maximum error in setting the gap distance is estimated to be less than 5%. A two-stage mechanical pump with a zeolite trap is used to evacuate the test gap. Ultimate pressure of both gaps as measured on an Alphatron gauge is in the range of 1 to 2×10^{-3} mm Hg. During measurements the test gas is admitted through a variable leak, and the pumping speed is reduced by a throttling valve. Thus, a small flow of gas through the test gap is ensured at all times. A standard mercury manometer is used as a check on the Alphatron gauge. Pressure measurements in the gap have an estimated accuracy of $\pm2\%$.

The 20-kV supply for the RG-8 line is fixed in output voltage so that adjustment of the air spark gap is unnecessary. The main pulse forming line is charged by a separate supply with variable output over the range 0 to 30 kV. Both supplies are 1% regulated and may be set to a given voltage with an average accuracy of $\pm2\%$. When the RG-17 pulse cable is charged to a voltage V_0 and discharged, the amplitude of the traveling wave is $V_0/2$. When the pulse reaches the test gap it is reflected back into the RG-17 coupling cable until such time as the test gap begins to conduct appreciable current. During the time that the traveling pulse is being reflected from the test-gap electrode the voltage across the gap is V_0. Measurement of the traveling pulse amplitude seen through the current-viewing resistor shows it to be $V_0/2$ within 1%. Hence, we have assumed that the voltage to which the pulse cable is charged is the voltage applied to the test gap and that losses in the high-pressure pulse generator are negligible. Rise time of the pulse depends on the particular voltage, the gas pressure in the pulse generator, and the electrode distance. Rise times of 0.25 to 1.0 nsec are observed. Ringing and overshoot are normally less than 10% of the average pulse amplitude.

MEASUREMENT TECHNIQUE

The meaningful interpretation of the breakdown data involves three experimental considerations which are applicable to all of the reported results. These are: the establishment of an operational criterion for the breakdown lag time based on the observed pulse shapes, the removal of the statistical variation from the lag-time data, and a consideration of departures from similarity for data obtained with differing combinations of the breakdown parameters.

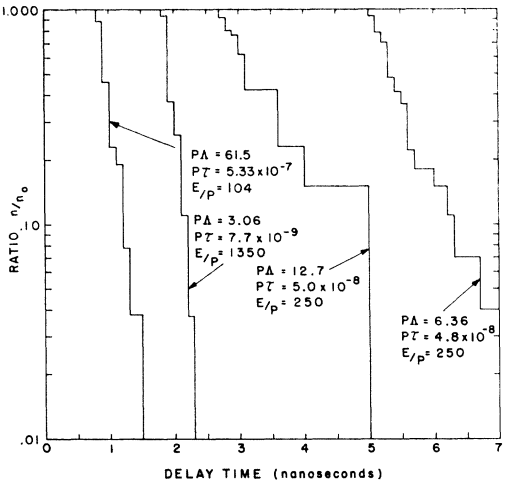

FIG. 6. Laue plots of statistical lags in air.

Figure 5 shows a typical pulse waveform provided by the current-viewing resistor (CVR) placed in the transmission line near the test gap. As the traveling wave passes the CVR the rise time of the wavefront AB is seen. As the wave continues passing the CVR and arrives at the gap the level portion BC is observed. When the wavefront reflected from the anode reaches the CVR (C to D on the trace) the waves traveling in two opposite directions cancel each other for a time given by DE. If breakdown does not occur in the gap the reflected wave continues and the trace is as shown in DEF. If breakdown takes place, the gap will begin to conduct after a short delay DE. When breakdown is fully formed, reflection from the gap ceases and the pulse height returns to its previous level as indicated by the portion GH.

For the purposes of this study the point E, indicating the onset of breakdown, is defined to correspond to a vertical deflection of one trace width above the base line of the trace. Further, we have measured formative time as the time between the instant the voltage reaches maximum on the anode (indicated by the point D in the observed pulse) and the time when the gap breaks down E.

The lag time DE is, in general, the sum of the formative and statistical lag times. The statistical delay time is caused by the finite rate of emission of electrons from the cathode surface and the statistical nature of the emission. Following the results of Strigel[11] and the analysis suggested by von Laue[12] the statistical time may be shown to obey an exponential distribution law. If the results of a number of measurements of the

[11] R. Strigel, Arch. Elektrotech. **26**, 803 (1932).
[12] M. von Laue, Ann. Physik **76**, 261 (1925).

TABLE I. Ranges of variables used for experiments.

Gas	Voltage range (kV)	Pressure range (mm Hg)	Gap distance (cm)	Purity (percent)	Measured formative time (nsec)
Air	5 to 30	1.0 to 760	0.13 to 6.0	Laboratory	0.5 to 18
Nitrogen	4 to 20	1.0 to 780	0.13 to 6.0	99.78	0.4 to 25
Oxygen	5 to 25	1.0 to 760	0.18 to 6.0	99.5	0.8 to 19
Argon	4 to 25	1.0 to 760	0.18 to 6.0	99.997	0.8 to 15
Helium	5 to 25	2 to 464	0.50 to 6.0	99.996	0.4 to 18
SF_6	4 to 25	1.0 to 750	0.051 to 6.0	98.7	0.4 to 19
Freon 12	7 to 25	1.0 to 500	0.051 to 6.0	99.9	0.3 to 11.5
Freon 114	7 to 25	1.0 to 760	0.051 to 6.0	99.9	0.4 to 17.5
Freon C318	7 to 25	1.0 to 700	0.051 to 6.0	99.5	0.8 to 11

delay time for fixed voltage, pressure, and gap distance are plotted on semilog axes with appropriate variables the exponential nature of the distribution may be seen. The statistical delay is described by

$$n_t = n_0 e^{-t/\sigma}, \tag{8}$$

where n_t is the number of time lags greater than t, n_0 is the total number of events, and σ is the mean statistical lag. Hence a semilog plot of n_t/n_0 versus t should be a straight line yielding a value for σ from the slope and a value for the minimum delay, or the formative time, from the intercept at $n_t/n_0=1$. Figure 6 shows four typical plots of actual measurements. Such plots have been made for all data reported here where use is made, on the average, of 27 data points for the measured lag time.

By the methods referenced above it is possible to use the information regarding σ to estimate the rate of electron emission from the ultraviolet irradiation of the cathode surface. Based on typical observed values of σ from the data the photoemission current for this experiment is approximately 5×10^{-10} A.

According to the theory, the formative time may be described in terms of the variables $P\tau$ and E/P as in Eq. (7). Similarity conditions should then apply in the sense that a particular value of E/P can be obtained from an unlimited number of combinations of the parameters: pressure, gap spacing, and pulse voltage. In our experiments we have made an attempt to check similarity relationships. Hence our breakdown curves show data for different gap distances at all places where it was possible to obtain such data within limits imposed by theory and the experimental equipment. The breakdown curves are then drawn through the average of values determined from measurements on gaps of 0.051 to 6.0 cm.

EXPERIMENTAL RESULTS

Breakdown measurements have been performed in a number of gases. Table I gives a summary of the laboratory variables used in the measurement of each gas as well as the nominal purity of each gas. The results of the present investigation are illustrated in Figs. 7 through 15 for the nine gases. These figures include the breakdown data with curves of the average measured results and the theoretically predicted curves where possible. The latter curves were derived from Eq. (7) by the methods described in Appendix I. Figure 16 summarizes the experimental breakdown results for all nine gases. For those gases where it has been possible to derive theoretical curves, generally good agreement between theory and experiment will be noted.

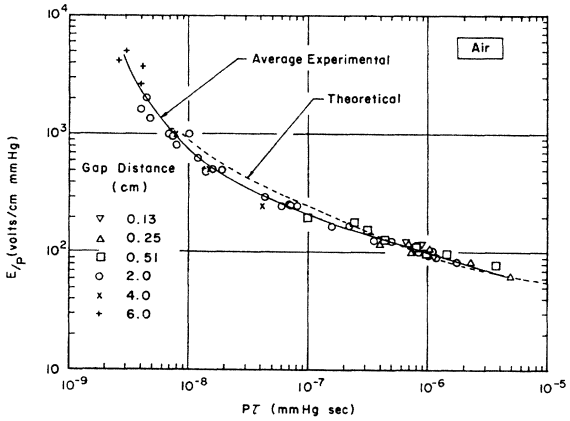

FIG. 7. E/P versus $P\tau$ for breakdown in air.

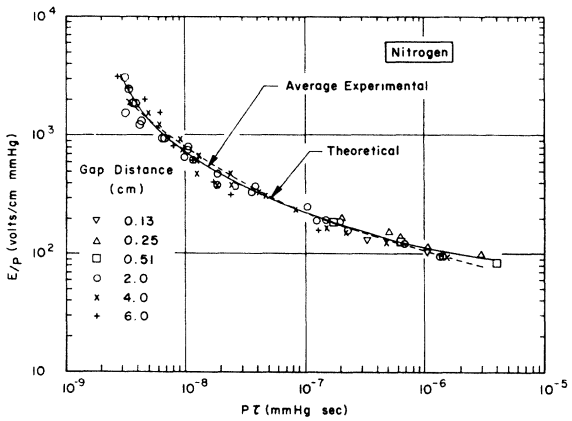

FIG. 8. E/P versus $P\tau$ for breakdown in nitrogen.

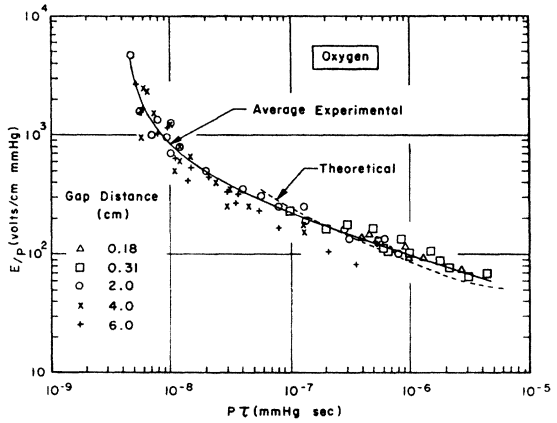

FIG. 9. E/P versus $P\tau$ for breakdown in oxygen.

The results in air are particularly interesting both because they may be compared with previous work and because they are of great practical interest. A detailed plot of our experimental results in air along with the air theoretical formative-time curve is shown in Fig. 7. The experimental curve is drawn through the average of the experimental points. Experimental breakdown data have been obtained for much higher E/P values than can be treated by the theory, owing to a lack of fundamental data at $E/P > 10^3$ V/cm mm Hg. The

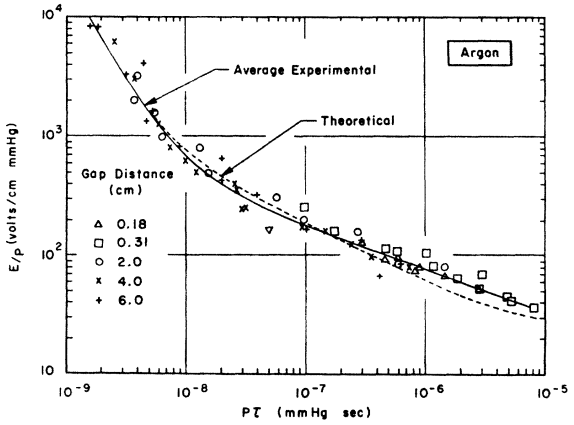

FIG. 10. E/P versus $P\tau$ for breakdown in argon.

data above this value are suggestive of an asymptotic approach to a minimum value of $P\tau$. It is plausible that this is brought about by an approach to conditions such that the collision frequency and ionization frequency are equal.

The results for nitrogen, oxygen, argon, and helium are plotted in a manner similar to that for air. Commercial quality gases were used in the experiments. The results of breakdown measurements in these gases are shown in Figs. 8 through 11.

Two sets of ionization coefficient data for helium are available (see Appendix I). Predictions based on these two sets of ionization data are shown in Fig. 11 along with the results of the present measurements. Agreement at the larger values of $P\tau$ is closest to predictions based on data of Druyvesteyn and Penning while at smaller values of $P\tau$ agreement is best with theory based on data of von Engel and Steenbeck. It is conjectured that this situation may be traced to similarities in gas purity between the referenced work and the present breakdown experiments. The breakdown measurements were carried out with impurities ranging from 1 part in 10^3 at values of $E/P > 500$ V/cm mm Hg to 1

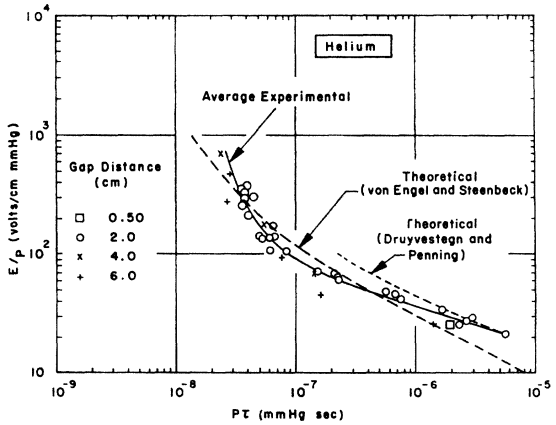

FIG. 11. E/P versus $P\tau$ for breakdown in helium.

part in 10^5 at lower values. The variation in purity was due to the experimental conditions of vacuum and continuous flow.

One interesting aspect of helium breakdown that has appeared in the experimental results is a reduction of breakdown pulse current for low pressures. For pressures of 1 mm Hg the equivalent gap impedance after the gap has broken down is many hundreds of ohms as against a fraction of an ohm under normal circumstances.

Results have been obtained in four insulating gases: Freon 114 ($CClF_2$-$CClF_2$); Freon C318 (C_4F_8 cyclic);

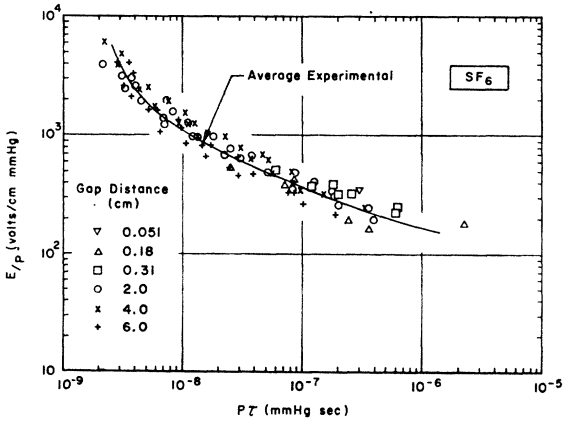

FIG. 12. E/P versus $P\tau$ for breakdown in sulphur hexaflouride.

Freon 12 (CCl_2F_2); SF_6. For all of these gases there exist insufficient data for the appropriate gas discharge parameters to make any theoretical predictions of breakdown. Hence for these gases we present only the experimental points and an average curve of the experimental points (Figs. 12–15).

SUMMARY

A theory has been developed for the formative period of dc-pulse breakdown in gases. Provided that the breakdown parameters are chosen within certain prescribed limits, the applicable theory is similar to the theory for microwave breakdown. To achieve the similarity the principal requirement is that which obviates a consideration of electrode and wall interactions and permits analysis of the breakdown formation in terms of gaseous processes alone. The resultant theory yields excellent agreement with previous measurements in air by both pulsed-dc and pulsed-microwave techniques and with the wide range of data achieved in the present research. Similar agreement is shown between theory and the present data for the several additional gases studied to the extent that the basic data are available for theoretical prediction of results.

In addition to providing information of direct applicability to problems in short-duration, high-voltage technology, the results given in this paper may be applied to high-power pulsed-microwave breakdown processes in a parameter range not previously reported. Further, by application of the analysis discussed in Appendix I, basic data regarding the net-ionization coefficient can be extracted for a range of the parameter E/P where measurement by other means does not exist.

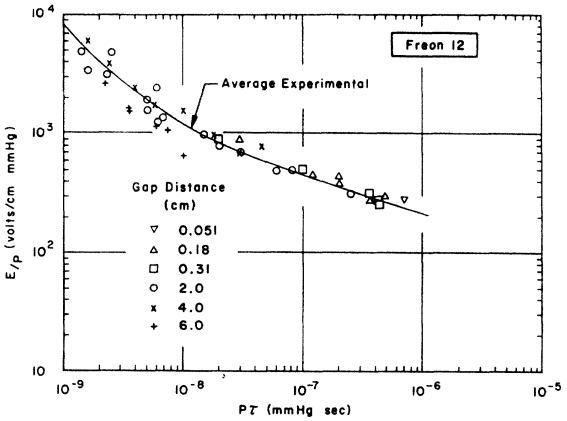

FIG. 13. E/P versus $P\tau$ for breakdown in Freon 12.

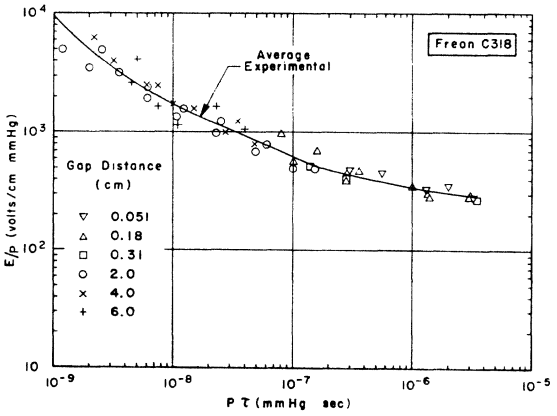

FIG. 14. E/P versus $P\tau$ for breakdown in Freon C318.

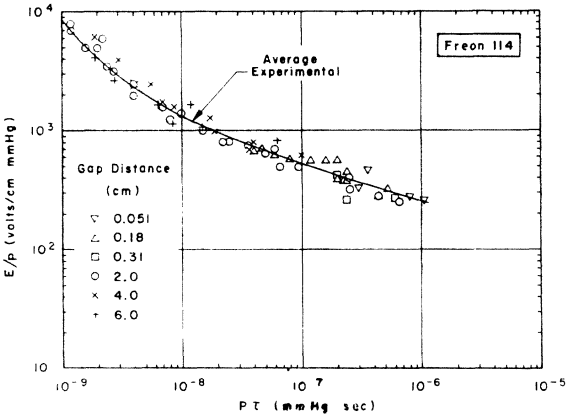

FIG. 15. E/P versus $P\tau$ for breakdown in Freon 114.

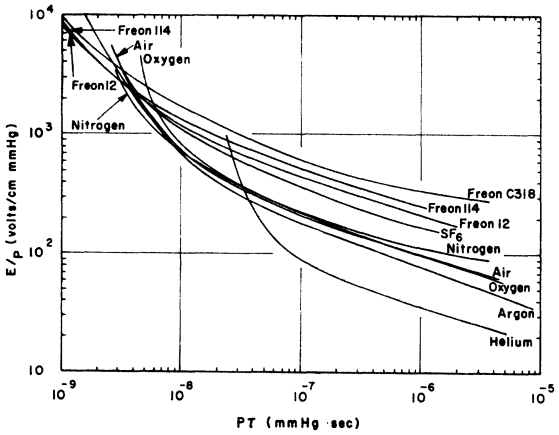

FIG. 16. Summary of formative-time measurements in nine gases.

ACKNOWLEDGMENTS

The authors gratefully acknowledge the interest and support of William C. Quinn and Ronald C. Blackall of Rome Air Development Center. They would also like to thank Wayne Kearsley for his efficient job of data reduction.

APPENDIX I: CALCULATION OF THEORETICAL BREAKDOWN CURVES

Theoretical breakdown curves have been calculated for five of the nine test gases. These curves are based

TABLE II. Gas-discharge parameters and references used to develop theoretical breakdown curves.

Gas	Range of applicable drift-velocity data (E/P)	Reference	Adopted linear extrapolation to drift-velocity data (cm/sec)	Range of net-ionization data (E/P)	Reference
Air	0.5–20	a	$7\times10^6+2\times10^5\ E/P$	50–67	b
	0.5–100	c		67–300	d
				300–1000	e
Nitrogen	40–200	f	$2.9\times10^5\ E/P$	40–100	g
				100–500	e
				500–2000	h
Oxygen	40–125	i	$14\times10^6+1.4\times10^5\ E/P$	40–66.7	b
				66.7–350	e
Argon	15–42	f	$10^6+2\times10^5\ E/P$	30–1500	d
Helium	0.5–45	j, k	$7.6\times10^5\ E/P$	10–100	d
				10–1000	l

[a] R. A. Nielson and N. E. Bradbury, Phys. Rev. **51**, 69 (1937).
[b] M. A. Harrison and R. Geballe, Phys. Rev. **91**, 1 (1953).
[c] J. S. Townsend, *Motions of Electrons in Gases* (Clarendon Press, Oxford, 1925).
[d] M. S. Druyvesteyn and F. M. Penning, Rev. Mod. Phys. **12**, 87 (1940).
[e] K. Masch, Arch. Elektrotech. **26**, 582 (1932).
[f] K. H. Wagner, Z. Physik **178**, 64 (1964).
[g] A. E. D. Haylen, Nature **183**, 1545 (1959).
[h] See Ref. 13.
[i] See Ref. 16.
[j] R. A. Nielson, Phys. Rev. **50**, 950 (1936).
[k] J. A. Hornbeck, Phys. Rev. **83**, 374 (1951).
[l] A. von Engel and M. Steenbeck, *Elektrische Gasentladungen* (Springer Verlag, Berlin, 1932), p. 106.

on Eq. (7) and available data in the manner outlined below.

Examination of the equation shows that a knowledge of two gas discharge parameters and the ratio of initial to final electron density are necessary for the calculation of $P\tau$-versus-E/P curves. Specifically, electron-drift velocity and net-ionization coefficients are needed as a function of E/P in order to calculate $P\tau$. Table II gives a summary of the range of E/P values for which drift-velocity and $(\alpha-\beta)/P$ data are available from the literature.

It is apparent from the table that the drift-velocity data are much more limited in range than the $(\alpha-\beta)/P$ data. We have therefore found it necessary to extrapolate the measured drift-velocity data. For this purpose we have plotted available drift-velocity data for the five gases versus E/P and have made a graphical linear extrapolation of the data. (Fortunately, for three of the gases we have very modern data[13,14] available from experiments done on a time scale similar to our own.) The analytic expression satisfying the linear extrapolation of existing drift-velocity data is shown in Table II for each of the five gases.

Not all available references containing net-ionization data were used because in many cases the differing references are not self-consistent. It may be noted that use has been made of both modern and older references. Where a choice was possible older references were used only for the high-E/P range. This is because the lack of good vacuum equipment and subsequent contamination (mercury vapor) is thought to have degraded results in many cases for measurements of α/P or $(\alpha-\beta)/P$ for low E/P. In all cases the ratio of initial to final electron density has been taken to be 10^8. This is in accord with results reported earlier.[4]

[13] A. von Engel, in *Handbuch der Physik*, edited by S. Flügge (Springer-Verlag, Berlin, 1956), Vol. 21, p. 504.
[14] L. Frommhold, Z. Physik **160**, 554 (1960).